JOURNAL OF GEOPHYSICAL RESEARCH, VOL. 111, E12S10, doi:10.1029/2006JE002754, 2006

Erosion rates at the Mars Exploration Rover landing sites and long-term climate change on Mars

M. P. Golombek,[1] J. A. Grant,[2] L. S. Crumpler,[3] R. Greeley,[4] R. E. Arvidson,[5] J. F. Bell III,[6] C. M. Weitz,[7] R. Sullivan,[6] P. R. Christensen,[4] L. A. Soderblom,[8] and S. W. Squyres[6]

Received 17 May 2006; revised 17 August 2006; accepted 22 September 2006; published 8 December 2006.

[1] Erosion rates derived from the Gusev cratered plains and the erosion of weak sulfates by saltating sand at Meridiani Planum are so slow that they argue that the present dry and desiccating environment has persisted since the Early Hesperian. In contrast, sedimentary rocks at Meridiani formed in the presence of groundwater and occasional surface water, and many Columbia Hills rocks at Gusev underwent aqueous alteration during the Late Noachian, approximately coeval with a wide variety of geomorphic indicators that indicate a wetter and likely warmer environment. Two-toned rocks, elevated ventifacts, and perched and undercut rocks indicate localized deflation of the Gusev plains and deposition of an equivalent amount of sediment into craters to form hollows, suggesting average erosion rates of ~0.03 nm/yr. Erosion of Hesperian craters, modification of Late Amazonian craters, and the concentration of hematite concretions in the soils of Meridiani yield slightly higher average erosion rates of 1–10 nm/yr in the Amazonian. These erosion rates are 2–5 orders of magnitude lower than the slowest continental denudation rates on Earth, indicating that liquid water was not an active erosional agent. Erosion rates for Meridiani just before deposition of the sulfate-rich sediments and other eroded Noachian areas are comparable with slow denudation rates on Earth that are dominated by liquid water. Available data suggest the climate change at the landing sites from wet and likely warm to dry and desiccating occurred sometime between the Late Noachian and the beginning of the Late Hesperian (3.7–3.5 Ga).

Citation: Golombek, M. P., et al. (2006), Erosion rates at the Mars Exploration Rover landing sites and long-term climate change on Mars, *J. Geophys. Res.*, *111*, E12S10, doi:10.1029/2006JE002754.

1. Introduction

[2] The geomorphology of a surface and the erosional and depositional processes that have acted on a surface provide clues to the climatic and environmental conditions that have affected it through time. At the first three landing sites on Mars (Viking Lander 1, Viking Lander 2, and Mars Pathfinder), the nature of features observed from the surface, when combined with the regional geologic setting of the landing sites derived from orbital data and ages from the density of impact craters, were used to infer the net change (erosion or deposition) as a means of quantifying the rates of geomorphic change. Because erosional and depositional processes that involve liquid water typically operate so much faster than eolian processes, the net change in the surface along with the presence or absence of process specific morphologies can be used to infer whether liquid water was involved and thus the climatic conditions. *Arvidson et al.* [1979] used Viking Lander 1 images of a crater rim to show that its rim height versus diameter ratio is close to that expected for a fresh crater in agreement with the population of fresh craters seen in orbiter images, thereby limiting the net erosion to less than a few meters over the lifetime of the surface. At the Viking Lander 2 site, inspection of the surface in concert with orbiter images of pedestal craters more loosely limited the amount of deflation to roughly 300 m over the lifetime of the surface [*Arvidson et al.*, 1979]. At the Mars Pathfinder landing site, the surface investigated by the lander and rover appears similar to that expected after formation by catastrophic floods and small net deflation of 3–7 cm is indicated by exhumed soil horizons, sculpted wind tails, pebble lag deposits and ventifacts [*Golombek and Bridges*, 2000]. Because all of

[1] Jet Propulsion Laboratory, California Institute of Technology, Pasadena, California, USA.
[2] Center for Earth and Planetary Studies, National Air and Space Museum, Smithsonian Institution, Washington, DC, USA.
[3] New Mexico Museum of Natural History and Science, Albuquerque, New Mexico, USA.
[4] Department of Geological Sciences, Arizona State University, Tempe, Arizona, USA.
[5] Department of Earth and Planetary Sciences, Washington University, St. Louis, Missouri, USA.
[6] Department of Astronomy, Cornell University, Ithaca, New York, USA.
[7] Planetary Science Institute, Tucson, Arizona, USA.
[8] U. S. Geological Survey, Flagstaff, Arizona, USA.

0148-0227/06/2006JE002754$09.00

these surfaces date from the Late Hesperian or Early Amazonian [*Tanaka et al.*, 2005], the inferred small net change over time coupled with the occurrence of only eolian erosional features argues that only the wind has acted on the surfaces and by inference that the climate has been dry and desiccating, similar to today, for the past ~3 Ga [*Hartmann and Neukum*, 2001].

[3] In contrast to the small changes to Hesperian and Amazonian surfaces visited by the Viking Landers and Mars Pathfinder, a wide variety of geomorphic indicators argue that certain older Noachian terrains were subject to a possible warmer and wetter environment in which liquid water was more stable than it is at present [e.g., *Carr*, 1996]. Many large Noachian craters are rimless and have shallow flat floors arguing they have been eroded and filled in by sediment [*Craddock and Maxwell*, 1993; *Grant and Schultz*, 1993; *Craddock et al.*, 1997]. Erosion of these craters, including many crater lakes [*Cabrol and Grin*, 1999; *Irwin et al.*, 2002, 2005; *Howard et al.*, 2005], and the formation of valley networks [*Baker et al.*, 1992] argue for relatively high erosion rates [*Grant and Schultz*, 1990; *Carr*, 1992; *Craddock and Maxwell*, 1993; *Craddock et al.*, 1997] involving liquid water, possibly driven by precipitation [*Craddock and Howard*, 2002; *Grant and Parker*, 2002; *Hynek and Phillips*, 2001]. The presence of widespread regularly layered sedimentary rocks and distributary, meandering channels have also been used to argue for the persistent flow of water and deposition in standing bodies of water in the Noachian [*Malin and Edgett*, 2000a, 2003]. These eroded Noachian terrains and sedimentary rocks argue strongly for early wet and possibly warm conditions, a scenario that is also supported by identification of phyllosilicates and sulfates in Noachian and layered terrain by OMEGA [*Bibring et al.*, 2006]. Because most of the valley networks trend down the topographic gradient produced by Tharsis loading in the Noachian (producing the negative gravity ring and antipodal dome that explains the first-order topography and gravity of the planet), volatiles released with the magma that created the Tharsis load might have led to an early warm and wet Martian climate [*Phillips et al.*, 2001].

[4] In this paper, we consider the surficial geology and geomorphology of the landing sites explored by the Mars Exploration Rovers (MERs), with context provided by mapping from orbit, to constrain the erosional and depositional processes that have acted on their surfaces. We make special use of impact crater morphology and morphometry, as fresh craters have a well-understood geometry and have been observed by the rovers at both landing sites. There are also a variety of craters in differing states of degradation at both sites. These observations allow us to place broad constraints on the types and vigor of erosional and depositional processes that have modified the surfaces, thereby constraining the environment and climatic conditions over time. We start by discussing the geologic setting from orbit and the surface geology from the rovers for each landing site, then derive erosion rates for each landing site, and finally discuss the results in terms of long-term climatic conditions over time. Our results support previous inferences that Mars likely had a warm and wet climate in the Noachian, but that a dry and desiccating environment similar to current conditions has been active for the Late Hesperian and all of the Amazonian.

2. Geology of Meridiani Planum

[5] The Mars Exploration Rover (MER) Opportunity landed in Meridiani Planum (Figure 1), a low-lying region of the heavily cratered highlands on the eastern edge of the western hemisphere of Mars [*Golombek et al.*, 2003]. Mapping of the area shows valley networks that trend northwest, down the topographic gradient that was created by the flexure surrounding Tharsis [*Phillips et al.*, 2001]. The region experienced extensive erosion and denudation that extended into the Late Noachian [*Hynek and Phillips*, 2001; *Grant and Parker*, 2002]. The Opportunity rover landed on plains that are near the top of a broad section of hundreds of meters thick layered, likely sedimentary materials [*Arvidson et al.*, 2003; *Hynek*, 2004; *Edgett*, 2005] (Figure 2), that disconformably overly the Noachian cratered terrain in this area [*Hynek et al.*, 2002; *Arvidson et al.*, 2003], but may be interbedded elsewhere [*Edgett*, 2005]. The layered rocks generally bury the valley networks in the cratered terrain, implying they are younger [*Hynek et al.*, 2002]. Measurement of the size-frequency distribution of a population of degraded craters >1 km in diameter clearly shows that the layered materials are also Noachian in age [*Lane et al.*, 2003; *Arvidson et al.*, 2006b], suggesting that the layered materials formed in the Late Noachian after the period of denudation that stripped the region. The apparent amount of material stripped from the highlands and the inferred rate of denudation prior to deposition of the layered materials suggest that precipitation and sapping or runoff may have been responsible during a wet and likely warmer climate in the Late Noachian [*Hynek and Phillips*, 2001; *Grant and Parker*, 2002].

[6] The plains surface that Opportunity has explored (Figure 2) is dominated by granule ripples formed by saltation induced creep of a lag of 1–2 mm diameter hematite spherules (called blueberries) underlain by a poorly sorted mix of fine to very fine basaltic sand [*Soderblom et al.*, 2004; *Sullivan et al.*, 2005; *Weitz et al.*, 2006]. The hematite spherules are concretions derived from the saltating sand eroding the underlying weak layered sulfate-rich sedimentary rocks [*Arvidson et al.*, 2004b; *Soderblom et al.*, 2004] (Figure 3) that form the top of the section of Late Noachian layered materials documented from orbit [*Hynek et al.*, 2002; *Arvidson et al.*, 2003; *Edgett*, 2005]. The underlying sedimentary rocks, known as the Burns formation are "dirty evaporites" that were likely deposited in acidic saline interdune playas [*Squyres et al.*, 2004; *Grotzinger et al.*, 2005; *Clark et al.*, 2005]. Sediments were subsequently reworked by wind and in some locations surface water and later underwent extensive diagenesis (including formation of the hematite concretions) via interaction with groundwater of varying chemistry [*McLennan et al.*, 2005]. The lower and middle units of the Burns formation likely were deposited by eolian dunes and sand sheets, respectively; the upper unit of the Burns formation includes small festoon cross beds that indicate deposition in flowing surface water [*Grotzinger et al.*, 2005]. By analogy with similar deposits on Earth that formed in saltwater playas or sabkhas, deposition of sediments of the Burns formation

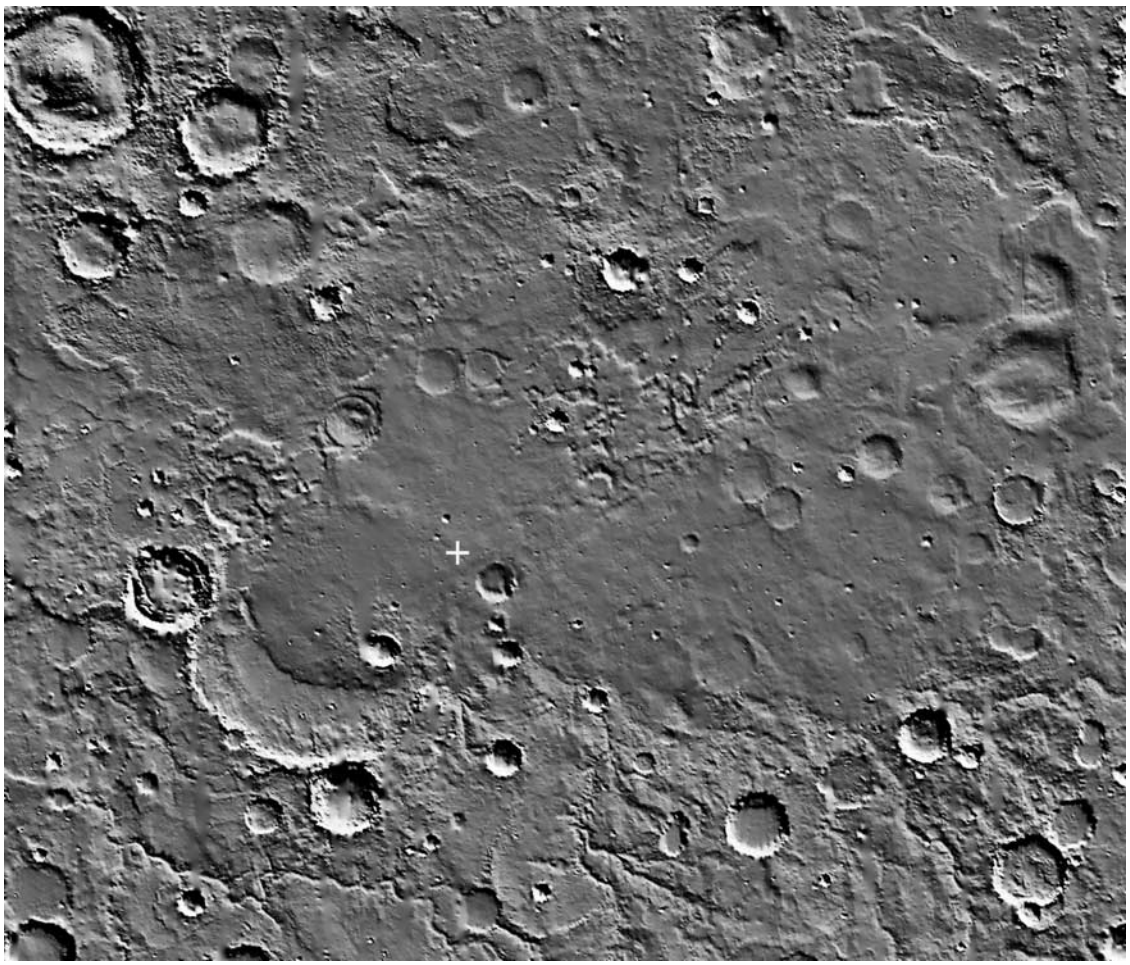

Figure 1. Regional setting of Meridiani Planum in shaded relief map derived from Mars Orbiter Laser Altimeter 128 gridded pixels per degree data. Note smooth, lightly cratered (Amazonian) plains on which Opportunity landed (cross), which bury underlying heavily cratered (Noachian) terrain with valley networks that trend to the northwest. Note large degraded craters in the smooth plains indicate the sulfate rocks below the basaltic sand and granule ripple surface are Late Noachian in age. Image is ~850 km wide; north is up.

probably occurred in a wet and likely warm environment in the Late Noachian on Mars.

[7] Eolian erosion of the weak sulfate bedrock is also revealed by a number of impact craters in a variety of stages of degradation that were visited by Opportunity (Figure 4). The craters observed range from fresh, relatively unmodified craters such as Vega, Viking and Fram to highly eroded and infilled craters such as Eagle and Vostok and document progressive eolian erosion of the weak sulfate bedrock and infilling by basaltic sand [*Grant et al.*, 2006a]. Counts of these craters including those <250 m in diameter, which are clearly sparse in orbital images (Figure 2), demonstrate that the average surface age of the basaltic sand and granule ripple surface is Late Amazonian [*Lane et al.*, 2003]. Furthermore, comparison of the measured crater density at Meridiani Planum with Hesperian age surfaces such as Viking Lander 1 and 2, Mars Pathfinder, and Gusev shows dramatically fewer craters. The dearth of craters at Meridiani argues that the entire Hesperian cratering record has been erased, further attesting to the erosion of older Noachian craters and terrain at Meridiani and of layered terrains in general [*Malin and Edgett*, 2000a; *Edgett*, 2005].

3. Surficial Geology in Gusev Crater

[8] The Mars Exploration Rover Spirit landed on the Gusev cratered plains [*Golombek et al.*, 2003]. The morphology of Gusev crater strongly suggests that a lake occupied the crater as a result of water and sediment discharge from the 800-km-long channel Ma'adim Vallis that drained through the highlands and breached the southern rim (with mesas interpreted to be deltas near the channel discharge area) [*Cabrol et al.*, 1998a, 1998b; *Irwin et al.*, 2002]. Mars Orbital Camera (MOC) images did not show obvious sedimentary layers on the floor of Gusev, but instead showed a cratered surface. Mapping and crater densities show the exposed Gusev floor formed near the beginning of the Late Hesperian [*Cabrol et al.*, 1998a; *Kuzmin et al.*, 2000; *Greeley et al.*, 2005] and is thus slightly older than Late Hesperian surfaces of the Viking 1 and Mars Pathfinder

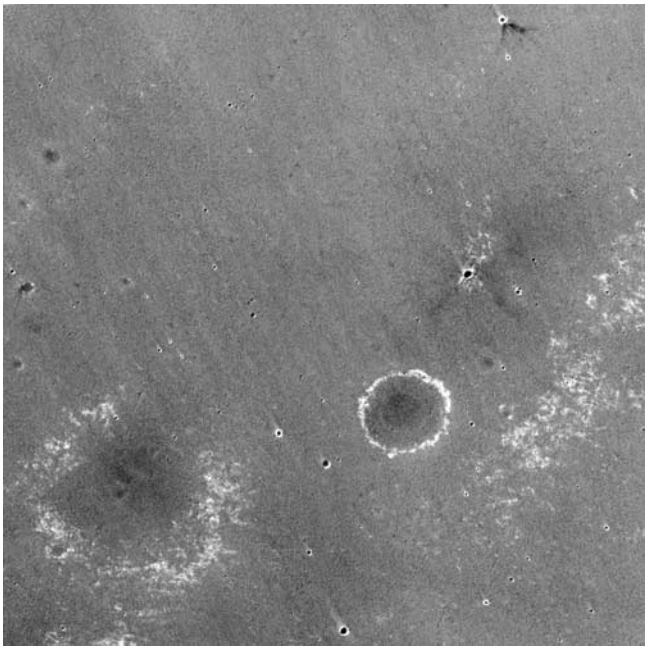

Figure 2. MOC image showing typical dark, smooth, basaltic sand surface and underlying light-toned sulfate evaporites in Meridiani Planum. Note lightly cratered surface age (Late Amazonian) and population of much older, highly degraded craters (bright rings) that date back to the Late Noachian. Note relatively fresh, small craters as well as more degraded, dark floored small craters that likely correspond to the gradational sequence documented by the rover (see text and Figure 4). MOC image E22-01660 is about 30 km west of the landing site and is about 2.6 km wide (north is up).

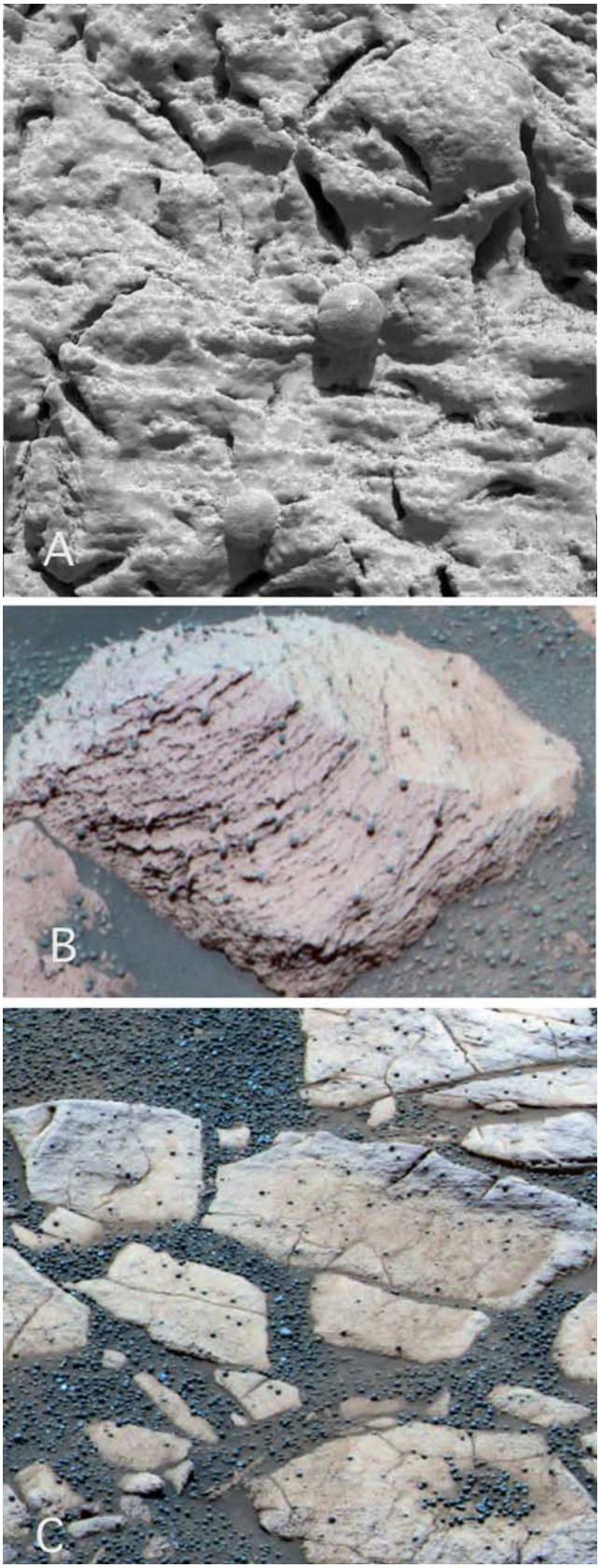

Figure 3. Hematite spherules in outcrop, weathering out of the outcrop as resistant spherules, and concentrated on the soil in Eagle crater and Meridiani Planum. (a) Microscopic Imager image of sulfate evaporites with hematite concretions. Note thin, horizontal laminations, vugs, and resistant concretions that are weathering out of the outcrop. Laminations are composed of sulfate sand deposited in an eolian or playa setting, vugs are dissolved crystal molds, and the spherules are hematite concretions that formed by diagenesis after deposition of the rocks. Image ID 1M130760791 is about 3 cm across. (b) Panoramic Camera (Pancam) image of the rock Pilbara near Fram crater showing stalks or barbs with blueberries at their ends. The blueberries are more resistant to erosion than the surrounding sulfates to saltating sand and thus weather out as coherent spheres that then litter the surface as a resistant layer of granules. (c) Pancam image showing the concentration of hematite concretions at the surface near the Berry Bowl and their relative paucity in the outcrop. Spherules are 1–6 mm in diameter and are not much smaller after weathering out of the outcrop, indicating they are generally resistant to erosion by the saltating basaltic sand. The hematite concretions are 1–4% by volume of the rock but are concentrated as a lag to roughly 10% by volume of the upper 1 cm of the sand.

and the early Early Amazonian surface of Viking 2 [*Tanaka et al.*, 2003, 2005].

[9] Spirit's observations of the surficial geology of the cratered volcanic plains at Gusev indicates they were modified chiefly by impact and lesser eolian activity [*Grant et al.*, 2004]. Spirit showed the plains are dominated by shallow circular depressions called "hollows," that have rocky rims and smooth, soil-filled centers (Figure 5). Perched, fractured and split rocks are more numerous around hollows than elsewhere and lighter toned (redder) rocks are more common near eolian drifts [*Grant et al.*, 2004]. Hollow morphology and size-frequency distribution indicate they are impact craters that were rapidly filled in by eolian material [*Grant et al.*, 2004; *Golombek et al.*, 2006]. Rocks are generally poorly sorted and angular and away from craters, pebbles appear embedded and cemented in the soil or perched above, suggestive of a crusted gravel armor or lag [*Greeley et al.*, 2004, 2006a].

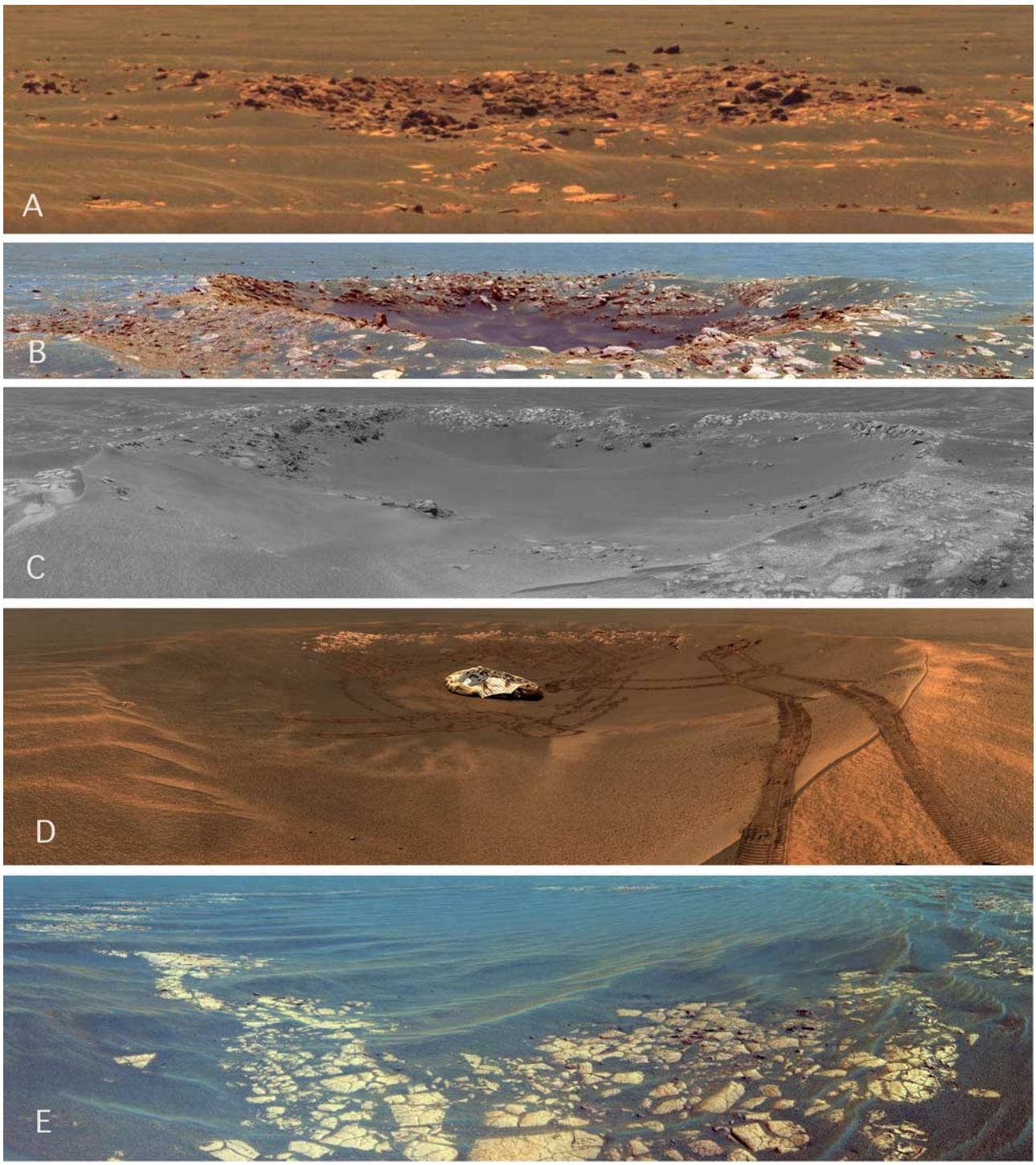

Figure 4

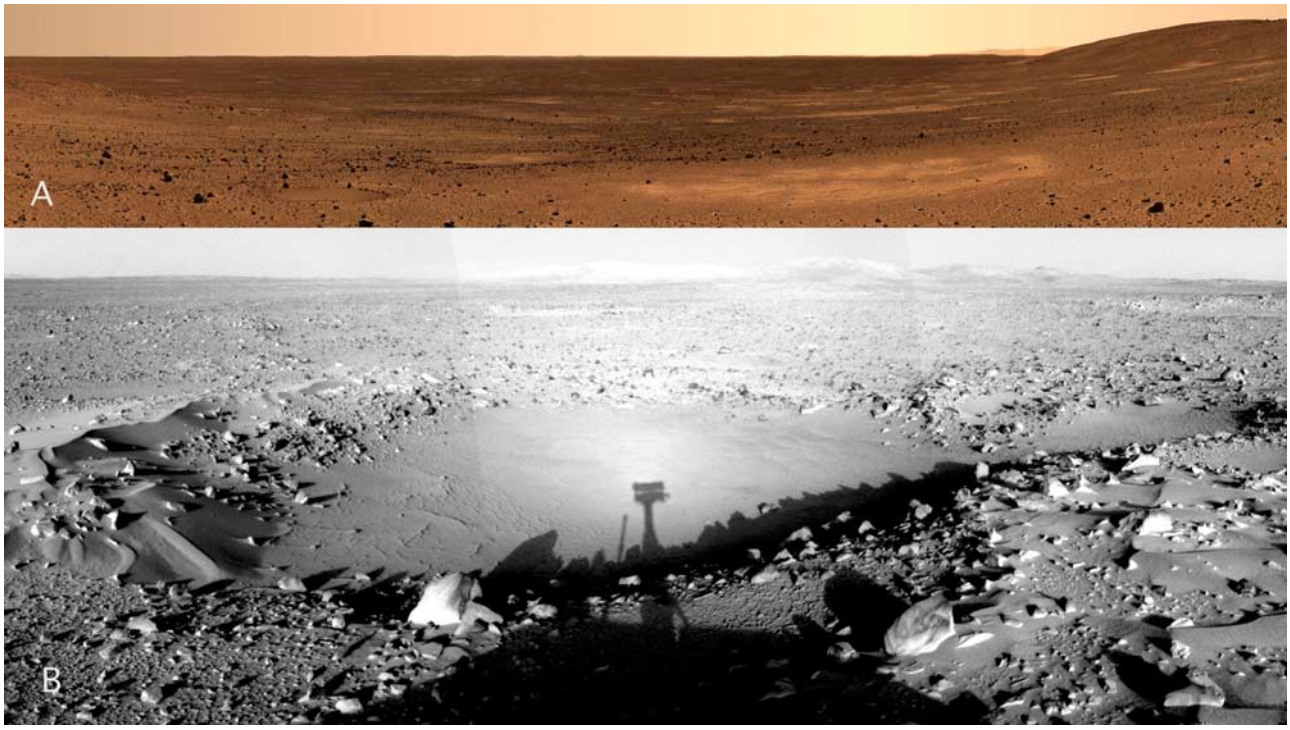

Figure 5. Images of hollows that characterize the Gusev cratered plains. Hollows are shallow soil-filled depressions typically with rocky rims. Their size-frequency distribution and morphology indicate that hollows are impact craters that have been filled in with sediment. (a) Pancam mosaic of Gusev cratered plain showing large number of circular soil filled hollows and rocky, desert pavement like plain. Portion of the Turkey Pancam panorama. (b) Navcam mosaic of sediment-filled hollows with rocky rims. Central larger hollow is 4.5 m in diameter with a rocky rim; smaller hollow to the right is about 2 m in diameter. Note shadow of the rover and imager. Note generally sediment starved view with few eolian drifts, rocky, pebble-rich lag surface and sediment-filled hollows, suggesting eolian redistribution of fines after cratering events to fill the closest depression. Navcam image mosaic 2NN111EFF36CYL00P1818L000M1.

[10] Spirit's observations of rock mineralogy, chemistry and texture (from microscopic images) revealed dark, fine-grained olivine basalts with thin coatings of dust and weathering rinds [*McSween et al.*, 2004, 2006; *Haskin et al.*, 2005]. The basalts appear to have been emplaced as relatively fluid lava flows [*Greeley et al.*, 2005] with vesicular clasts and rare scoria similar to inflated lava flow tops [*Crumpler et al.*, 2005; *Golombek et al.*, 2006]. Observations of the interior of the relatively fresh crater Bonneville indicate that it impacted into a rubble layer locally up to 10 m thick, likely derived from impact gardening of the basalt flows [*Grant et al.*, 2004, 2006a; *Golombek et al.*, 2006].

[11] The reddish soils appear to be weakly cemented fines with sand and granules that have been sorted into eolian bed forms [*Greeley et al.*, 2004, 2006a]. Bed forms consist primarily of meter-size ripples in which the crests have a surface layer of subangular to rounded granules and the troughs consist of poorly sorted fine to coarse sand. The sand does not appear to be currently active, based on the presence of surface crusts and dust cover on the bed forms and the absence of sand dunes and steep slip faces [*Greeley et al.*, 2004, 2006a].

[12] Many of the rocks at Gusev show evidence for partial or complete burial, followed by exhumation [*Grant et al.*, 2004; *Greeley et al.*, 2004, 2006a] (Figure 6). These include

Figure 4. Rover images of small, young craters on Meridiani Planum in various states of degradation by saltating basaltic sand. All impacts expose underlying sulfates and range from fresh (top) with blocky ejecta and little sand fill to highly degraded (bottom) with completely planed off ejecta and filled in centers. (a) Color Pancam mosaic of fresh, 8 m diameter Vega crater, which has fresh blocky ejecta and little sand fill (>0.5 m deep). Only some ejecta blocks (foreground) have been planed off. (b) False color Pancam mosaic of the relatively fresh, 15 m diameter Viking crater, with blocky rim, planed off ejecta and minor sand fill (3 m deep). (c) Navigation Camera (Navcam) mosaic of partially degraded 18 m diameter Voyager crater, with completely planed off ejecta, more subdued rim and significant sand fill (~1 m deep). (d) Color Pancam mosaic of highly degraded 22 m diameter Eagle crater, with ripple covered rim, sand fill (2 m deep), and little exposed outcrop. Note lander inside crater and sulfate outcrop on far side that Opportunity studied for the first 50 sols of the mission. (e) False color Pancam mosaic showing highly degraded 40 m diameter Vostock crater that has been almost completely filled in with basaltic sand (<1 m deep), leaving a ring of flat-lying bright blocks of sulfate that have been completely planed off.

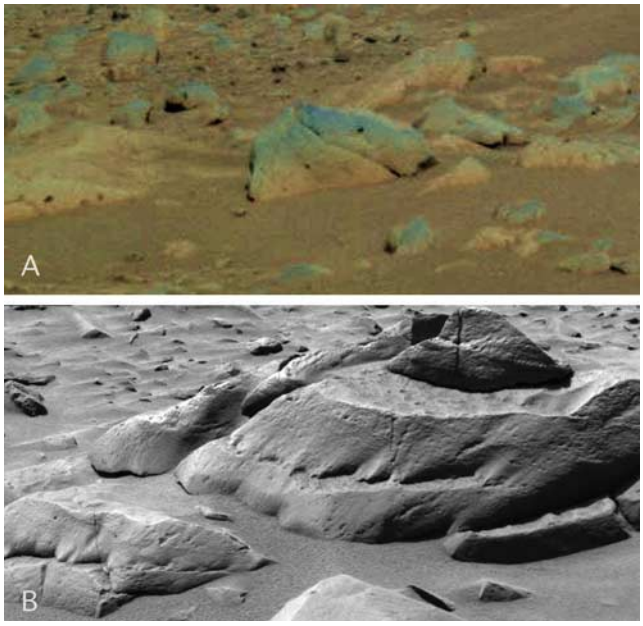

Figure 6. Evidence for deflation of the cratered plains surface. (a) Pancam image of two-toned rocks with redder patination along their bases, suggesting about 10 cm of deflation. Largest rock is about 35 cm wide. (b) Rocks showing ventifacts at common horizon about 8 cm above their bases, indicating burial when eroded by saltating sand and later deflation. Pancam image 2P131954281SFL1300P2531L7M1 of Terrace rock.

two-toned rocks with a redder patination along their bases, ventifacts that originate from a common horizon above the soil (suggesting that the lower part of the rock was shielded), rocks that appear to be perched on top of other rocks, and some undercut rocks, in which the soil has been removed around their bases. In places where clear evidence for localized deflation is seen, estimated depths of deflation range from 5 to 27 cm [*Greeley et al.*, 2006a]. No unambiguous obvious evidence for repeated burial and exhumation of the surface (e.g., multiple ventifact horizons) has been seen, but neither can it be ruled out [*Grant et al.*, 2004; *Greeley et al.*, 2004, 2006a; *Golombek et al.*, 2006]. Regardless of whether there has been repeated burial and exhumation on small scales (accompanying, for example, migration of an eolian bed form), the total deflation since formation of the observed hollows has not substantially exceeded a few tens of centimeters.

[13] Our interpretation is that excavation during impact deposited ejecta with widely varying grain sizes and fractured rocks, whose fine fraction was in disequilibrium with the eolian regime [*Grant et al.*, 2004]. Deflation of the ejected fines exposes more fractured rocks, and created a population of perched coarser fragments. The transported fines are trapped within nearby depressions (craters) creating the hollows [*Golombek et al.*, 2006]. Trenching in Laguna hollow near the edge of the Bonneville ejecta exposed unaltered basaltic fines capped by a thin layer of brighter, finer, globally pervasive dust [*Arvidson et al.*, 2004a]. The lack of evidence for dust in the subsurface soil in the hollows coupled with their uniformly filled appearance implies relatively rapid modification with locally derived sediment to their current more stable form [*Grant et al.*, 2004].

[14] Spirit traversed from the cratered plains into the older Columbia Hills on Sol 156 [*Arvidson et al.*, 2006a]. The cratered plains, surround and embay the Columbia Hills in accord with the interpretation that the cratered plains are impact modified basalt flows [*Crumpler et al.*, 2005; *Golombek et al.*, 2006]. Mapping and crater counts of morphologic units inside Gusev crater indicate the Columbia Hills are Early Hesperian in age [*Kuzmin et al.*, 2000; *Greeley et al.*, 2005]. Rocks that make up the Columbia Hills (as opposed to the geomorphic surface mapped from orbit) show strong chemical and mineralogic evidence for aqueous processing [*Ming et al.*, 2006; *Morris et al.*, 2006; *Squyres et al.*, 2006], consistent with an early wet period in Mars history. The existence of "exotic" ejecta on Husband Hill not present on the plains argues for the emplacement of this ejecta on the surface prior to cratered plains basalt flooding and the persistence of the ejecta to the present limits the total erosion to of order meters since the Early Hesperian [*Grant et al.*, 2006b].

4. Erosion Rates at Gusev Crater

[15] The observed redistribution of 5–27 cm of ejected fines across the Gusev cratered plains represents the cumulative change of the surface since basalt flows formed the surface at the beginning of the Late Hesperian, or ~3.5 Ga [*Greeley et al.*, 2005]. This net gradation provides an estimate of the average rate of erosion or redistribution via the vertical removal of material per unit time, typically measured on Earth in Bubnoff units (1 B = 1 μm/yr) [*Saunders and Young*, 1983]. An average 10 cm of deflation or redistribution at the site (Table 1) yields extremely slow average erosion rates of ~0.03 nm/yr or between 0.01 nm/yr and 0.08 nm/yr (of order 10^{-5} B, where 1 B equals 1 μm/yr, which equals 10^3 nm/yr).

[16] Deflation and redistribution of a single layer of fines about 10 cm thick would also fill all the hollows observed via the following test. From the measured size-frequency of craters and hollows [*Golombek et al.*, 2006], we selected a matching distribution of craters in an example 1 km^2 area yielding about 2000 craters ranging from ~100 m to 2 m diameter. Next, all craters were assumed to have a fresh shape similar to Bonneville (the freshest crater observed by Spirit), with a depth/diameter ratio of 0.1 and 15° wall slopes [*Grant et al.*, 2004, 2006a]. As argued by *Golombek et al.* [2006] and *Grant et al.* [2006a], this shallow depth/diameter ratio is consistent with the craters being secondaries with relatively minor modification rather than primaries with extensive modification. The flat floor and constant wall slopes are consistent with a class of small, fresh lunar craters [*Wood and Andersson*, 1978] that appear to be the primary shape that then degrade into bowl shaped craters [*Ravine and Grieve*, 1986]. The volume of the craters was calculated by differencing the volume of 2 cones, one with the diameter of the crater $[(D_c/2)\ \pi\ \tan\alpha\ (D_c/2)^2]/3$ and the other with the diameter of the floor $[(D_f/2)\ \pi\ \tan\alpha\ (D_f/2)^2]/3$, where the diameter of the crater floor, $D_f = D_c - [2d/\tan\alpha]$, the crater depth, $d = 0.1\ D_c$, and D_c is the diameter of the crater, and α is the wall slope.

Table 1. Summary and Derivation of Average Erosion Rates on Mars

Stratigraphic Series[a]	Age,[b] Ga	Estimated Time, Ga	Erosion, m	Average Erosion Rate, nm/yr	Method	Source	Key to Figure 7
Middle–Late Noachian	3.95–3.7	0.25	200	800	crater degradation	*Craddock et al.* [1997]	tan, solid
Middle–Late Noachian	3.95–3.7	0.25	250	1000	crater degradation	*Hartmann et al.* [1999]	brown, solid
Middle Noachian-Hesperian	3.95–3.0	0.95	290–2300	1295	crater degradation	*Craddock and Maxwell* [1993]	grey, solid
Late Noachian	3.83–3.7	0.13	1000	7700	Meridiani denudation	*Hynek and Phillips* [2001]	black, solid
Late Noachian	3.83–3.7	0.13	1000	7700	crater degradation	*Carr* [1992]	orange, solid
Hesperian-Amazonian	3.7–0	3.7	65	18	crater degradation	*Carr* [1992]	orange, dashed
Late Hesperian-Amazonian, Gusev[c]	3.6–0	3.6	3	0.8	deflation of Husband Hill	*Grant et al.* [2006b]	light green, solid
Beginning of Late Hesperian–Amazonian, Gusev[d]	3.5–0	3.5	0.05–0.27	0.03	deflation of landing site, cratered plains	this study	rose, solid
End of Late Hesperian –Amazonian, VL1[e]	3.2–0	3.2	3	1	fresh crater rim height	*Arvidson et al.* [1979]	light blue, solid
End of Late Hesperian - Amazonian, MPF[e]	3.1–0	3.1	0.03–0.07	0.02	deflation of landing site	*Golombek and Bridges* [2000]	dark blue, solid
Amazonian, VL2[e]	3.0–0	3.0	300	100	pedestal crater deflation	*Arvidson et al.* [1979]	violet, dashed
Amazonian, Meridiani	3.0–0	3.0	10–80	15	loss of Hesperian craters	this study	purple, solid
Late Amazonian, Meridiani	0.4–0	0.4	1–10	12.2	degradation of fresh craters	this study	red, solid
Late Amazonian, Meridiani	0.4–0	0.4	0.5	1.3	concentration of blueberry surface lag	this study	pink, solid

[a]Stratigraphic series from *Tanaka* [1986].
[b]Time of series from *Hartmann and Neukum* [2001].
[c]Age of site from *Kuzmin et al.* [2000].
[d]Age of site from *Greeley et al.* [2005].
[e]Age of site from *Tanaka et al.* [2005].

[17] The volume of all 2000 craters was then related to the thickness of a uniform surface layer over the 1 km^2 area that would fill the craters. The result is that a layer of material roughly 10 cm thick (with a volume of ~100,000 m^3) would fill the craters. This matches the average estimate of deflation from two-toned rocks and elevated ventifacts of ~10 cm and argues that little has happened at the site except periodically high deflation (following impacts) of locally derived surface fines to fill the impact craters and create the hollows. Again, this argues for extremely slow average long-term erosion rates.

[18] The persistence of exotic ejecta on Husband Hill emplaced prior to the basalt flows of the cratered plains, limits erosion of the Columbia Hills to of order meters [*Grant et al.*, 2006b] since the mapped surface age of Early Hesperian. Erosion of several meters of material since the end of the Early Hesperian (3.6 Ga [*Hartmann and Neukum*, 2001]), yields erosion rates of ~0.8 nm/yr for Husband Hill.

5. Erosion Rates at Meridiani Planum

[19] Slightly higher Amazonian erosion rates are implied at Meridiani Planum [*Soderblom et al.*, 2004; *Arvidson et al.*, 2004b] (and other exhumed Noachian layered terrains on Mars [*Malin and Edgett*, 2000a; *Edgett*, 2005; *McEwen et al.*, 2005]). The loss of Hesperian craters indicated by the measured size-frequency distribution of craters records erosion loosely bracketed between 10 m and 80 m based on the following argument. *Arvidson et al.* [2006b] measure a decrease in the number of craters smaller than ~400 m diameter associated with the loss of Hesperian craters. A fresh primary crater 400 m diameter is roughly 80 m deep (from the 0.2 depth/diameter ratio of small fresh craters [*Pike*, 1980; *Wood and Andersson*, 1978]), so to erode craters 400 m and smaller requires removal of ~80 m of material. This represents the maximum erosion as more erosion would remove larger craters than 400 m diameter, which is not observed in the measured size-frequency distribution [*Arvidson et al.*, 2006b]. If, however, not all the craters are removed but instead many are filled in, less material can be removed. Because Opportunity has visited relatively intact sections of outcrop, at least the ejecta of the Hesperian craters must have been removed. From the Gusev cratered plains and the observed rubble layer in the wall of Bonneville crater, we estimate the ejected layer of Hesperian craters could be ~10 m thick [*Grant et al.*, 2004; *Golombek et al.*, 2006]. Loss of 10–80 m of material at Meridiani Planum since the Hesperian (~3.0 Ga [*Hartmann and Neukum*, 2001]), suggests erosion rates of 3.3–26.7 nm/yr (Table 1). We note that higher erosion rates are expected in weak, easily erodible deposits [e.g., *Maxwell and Irwin*, 2004] and higher erosion rates are consistent with very lightly cratered layered deposits on Mars in general [*Malin and Edgett*, 2000a; *McEwen et al.*, 2005].

[20] Estimates of erosion rates derived in this manner are comparable with those resulting from the observed erosion and modification of young craters and ejecta by the saltating Meridiani sand (Figure 4). The hematite bearing plains have very few impact craters and counts of small craters indicate a surface age of Late Amazonian [*Lane et al.*, 2003]. In high-resolution images (e.g., Mars Orbiter Camera) the craters appear fresh (Figure 2), but observations by Oppor-

tunity suggest they are being eroded and modified by the saltating sand. The sulfate evaporites are weak (inferred from the grind energy needed by the Rock Abrasion Tool [*Arvidson et al.*, 2004b] and the observed hematite spherule blueberry "stalks" or ventifacts) and easily erodible by the saltating sand [*Soderblom et al.*, 2004; *Grant et al.*, 2006a]. Opportunity visited about a dozen craters in various stages of erosion and modification (Figure 4). The freshest crater, Vega, has a blocky rim and a rocky ejecta blanket and does not have sand ripples that overtop the rim. Slightly more eroded craters such as Viking, Voyager and Fram still have blocky rims and rocky ejecta, but much of the ejecta is planed off level with the surface and their interiors have been partially filled with sand. It is noteworthy that sulfate rocks at Fram have particularly well exposed blueberry "barb" or "stalk" ventifacts (Figure 3b) near planed off ejecta blocks. Craters such as Naturaliste and Géographe are characterized by ejecta and rim relief that is planed to the level of the sand and ripples cover their rims and sand fills their interiors. More eroded craters such as Endurance, Eagle, Jason and Alvin have no ejecta (completely eroded away), have back-wasted and eroded rims and have interiors with significant deposits of sand. Finally, the rim of Vostok has been almost completely eroded (expressed as a very low ring of planed-off sulfate blocks) and the interior is almost completely filled. This degradational sequence shows that so-called "fresh craters" in orbital images constitute a sequence of craters in various states of erosion and infilling (Figures 4 and 2).

[21] Consideration of current crater diameters, original fresh crater depths, and ejecta thicknesses [*Grant et al.*, 2006a], and the amount of erosion and infilling needed to produce the observed modification of craters bounds the amount of erosion to between 1 and 10 m. For example, Vostok, the most eroded crater, is about 45 m in diameter and retains only about a meter of relief at most, so about 8 m of sand would fill it if it was a primary crater with an original depth/diameter ratio of 0.2 [*Pike*, 1980; *Wood and Andersson*, 1978] (Figure 4). The largest crater, Endurance, is 150 m diameter, has had its ejecta blanket (estimated to be ~2 m thickness) eroded away, suffered back wasting of its rim by 5–10 m, and had about 5 m of sand deposited in its interior [*Grant et al.*, 2006a, 2006b]. All the other craters are less than ~22 m diameter and record erosion and back wasting of their rims and ejecta, and deposition of sand in their interiors of 1–5 m. More than 10 m of erosion would have completely erased some of these craters, so that represents the maximum erosion, and less than 1 m of erosion would not have modified others, so that represents the minimum. Erosion of 1–10 m needed to modify the craters over the Late Amazonian age of the surface (~400 Ma [*Hartmann and Neukum*, 2001]), yields erosion rates of 2.5–25 nm/yr (Table 1), which are comparable to those estimated from the loss of Hesperian craters.

[22] The concentration of hematite-rich spherules (so called blueberries) on the surface as a granule lag [*Soderblom et al.*, 2004; *Sullivan et al.*, 2005; *Weitz et al.*, 2006], also yields comparable erosion rates. The blueberries make up only 1–4% of the volume of sulfate outcrop exposed in Eagle, Fram and Endurance craters [*McLennan et al.*, 2005], but make up about ~10% of the volume of the upper 1 cm of the sand [*Soderblom et al.*, 2004] (Figure 3). For a 1% volume in the outcrop to produce a 10% volume in the upper 1 cm requires about 10 cm of erosion. However, this estimate assumes that the volume fraction of blueberries within the overlying strata that eroded away was the same as in the outcrop observed below. Sulfate sedimentary rocks at Erebus crater appear blueberry free (blueberry size in the outcrop and soils decreases to the south from Endurance crater [*Weitz et al.*, 2006]), so it is possible that more rock eroded but did not leave as many blueberries behind. Also some angular, smaller and likely eroded blueberries are also present in the soil at the surface, suggesting that although the hematite-rich concretions are more resistant to erosion than the sulfate outcrop, some fraction of the concretion population may be eroding with time [*Soderblom et al.*, 2004; *Weitz et al.*, 2006]. In an example scenario, if the total erosion of sulfates needed to produce the blueberry concentration near the surface were increased to 50 cm, the indicated erosion rate would be only 1.3 nm/yr (Table 1) in the Late Amazonian (~400 Ma). This calculation could represent a minimum, but given the inherent uncertainties, it appears more poorly constrained than the other estimates.

6. Discussion

[23] Long term average erosion rates during the Hesperian and Amazonian from deflation and filling of craters in the Gusev plains and those derived from erosion of Hesperian craters, modification of Amazonian craters, and the concentration of hematite-rich spherules in the soils of Meridiani (Table 1) are so low (Figure 7) that they indicate a dry and desiccating climate similar to today's for the past 3.5 Ga. These erosion rates vary from order 0.01 to 10 nm/yr and are 2–5 orders of magnitude below the slowest continental denudation rates on the Earth [*Judson and Ritter*, 1964; *Saunders and Young*, 1983; *Summerfield*, 2005]. Stable cratons and passive continental margins on Earth have recorded denudation rates as low as a few Bubnoff units (μm/yr) [*Summerfield*, 2005]. Although slower erosion rates have been reported in the literature for cratons of Gondwanaland [*King*, 1962; *Twidale*, 1978; *Fairbridge and Finkl*, 1980; *Young*, 1983], quantitative apatite fission track data have shown rates of 10–1000 B for the Gondwanaland margins of Australia [*Bishop and Goldrick*, 2000], South America [*Brown et al.*, 2000] and Africa [*Brown et al.*, 2002]. The slowest erosion rates on Earth are recorded in both wet and dry environments without significant relief and are typically 10–100 B (10^4–10^5 nm/yr) [*Saunders and Young*, 1983; *Judson and Ritter*, 1964]. They are calculated over hundreds of millions of years time intervals (generally comparable to those determined on Mars) and are determined for low-relief areas similar to existing landing sites on Mars.

[24] Average erosion rates determined for the Gusev cratered plains (0.03 nm/yr) are comparable to those estimated in a similar manner for the Mars Pathfinder landing site (~0.02 nm/yr) [*Golombek and Bridges*, 2000] and for the Viking Lander 1 site (~1 nm/yr) [*Arvidson et al.*, 1979] and argue for very little net change of these surfaces throughout the Amazonian and much of the Late Hesperian [*Golombek and Bridges*, 2000] or since ~3.5 Ga [*Hartmann and Neukum*, 2001] (Table 1 and Figure 7). These rates are so low that taken literally they indicate an average loss of a

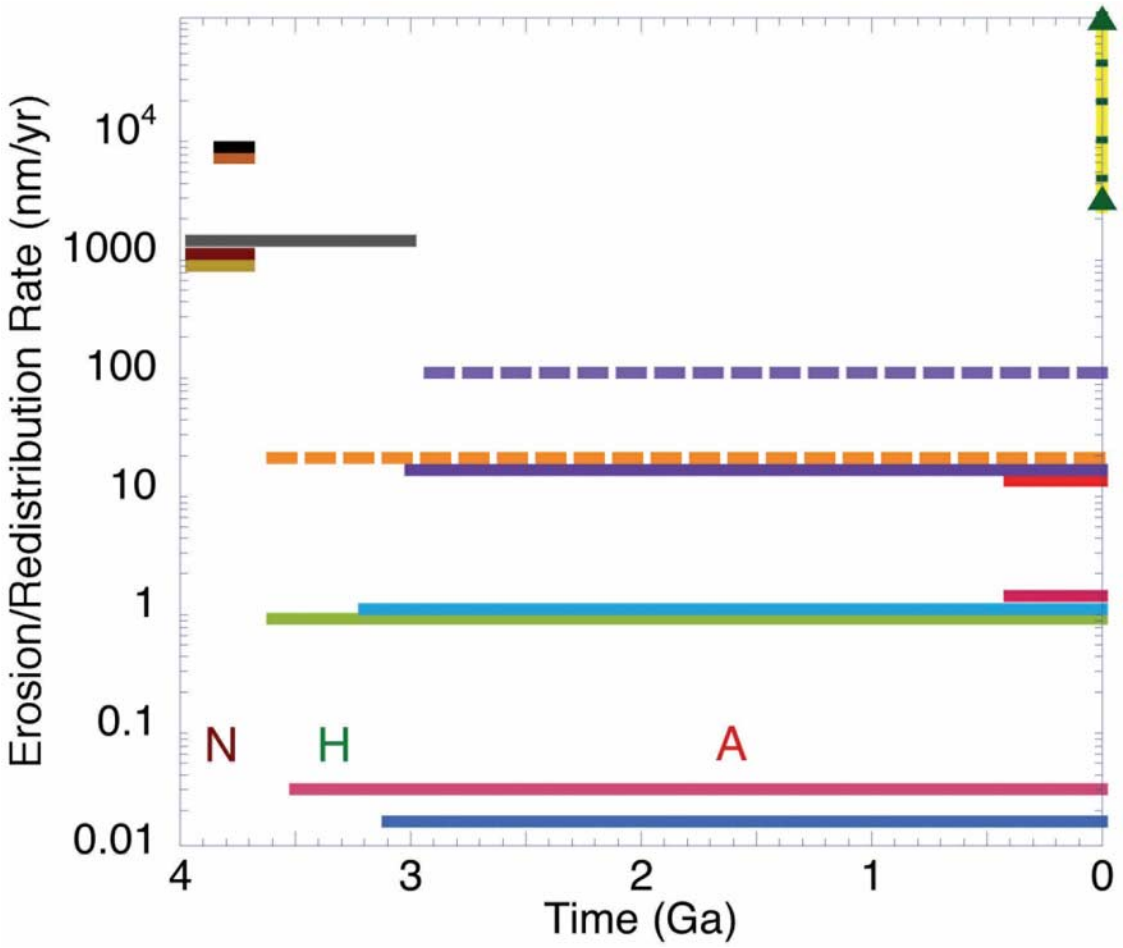

Figure 7. Erosion and redistribution rates versus time for the Spirit and Opportunity landing sites compared with other landing sites and terrains for the three epochs of Mars history: Noachian (N) >3.7 Ga, Hesperian (H) 3.7–3.0 Ga, and Amazonian (A) <3.0 Ga [*Hartmann and Neukum*, 2001]. Average erosion rates derived from the sources in Table 1 (includes the key for each estimate shown) have been recalculated for this timescale: Noachian are rates in black, orange, brown and tan; Noachian-Hesperian rate is in gray; Late Hesperian through Amazonian rates are in blue, rose, purple, and green (and dashed); and Late Amazonian rates are in pink and red. Vertical green and yellow rates with arrow end points are present-day slow continental denudation rates on Earth and present-day dust deposition and removal rates (~2–100 B), respectively, on Mars from the rovers and as inferred from dust devils observed by Spirit (see text for discussion and references). Average erosion rates from Noachian terrains on Mars are comparable to slow continental denudation rates on Earth, suggesting a wet and warm environment. Average erosion rates after the Hesperian are 2–5 orders of magnitude lower and are consistent with the dry and desiccating environment of today.

layer about a one atom thick per year from the surface. In reality, this very low net erosion is almost certainly a result of more rapid cycles of erosion, mantling and deflation that occurred over shorter periods. These cycles would be followed by no further erosion yielding the extremely slow calculated long-term rates. Further, the rates likely represent redistribution or localized deflation rather than true denudation, although they can be compared to average erosion rates as a coarse indicator of the climatic conditions active since the Hesperian. The calculated deflation rates for the Viking 1, Pathfinder and Spirit landing sites are about 3–5 orders of magnitude below the slowest erosion rates on Earth [*Saunders and Young*, 1983] and argue that liquid water was not an active erosional agent at these locations.

[25] Average erosion rates indicated from the loss of Hesperian craters, degradation of Late Amazonian craters, and concentration of hematite concretions from the Late Noachian evaporites at Meridiani Planum are around 1–10 nm/yr (Table 1 and Figure 7). These erosion rates are slightly higher than those estimated from the Viking 1, Pathfinder and Spirit landing sites, but higher erosion rates are expected in weak, easily erodible deposits [e.g., *Maxwell and Irwin*, 2004] like the Meridiani sulfates and such higher erosion rates are consistent with the very lightly cratered layered deposits on Mars in general [*Malin and Edgett*, 2000a; *McEwen et al.*, 2005]. Even so, these erosion rates are about 2–3 orders of magnitude lower than the slowest erosion rates on Earth (including the centers of low-relief

cratons calculated over comparably times) involving liquid water [*Saunders and Young*, 1983].

[26] Average erosion rates of 0.01–10 nm/yr contrast greatly with the rapid redistribution or cycling of dust (Figure 7) from the atmosphere to the surface and then back into the atmosphere (often leaving little trace on the surface). Mars Pathfinder and the two MERs measured maximum dust accumulation over extended periods of 0.29% per day [*Landis and Jenkins*, 2000; *Arvidson et al.*, 2004a, 2004b], which translates to a deposition rate of order 10^4 nm/yr [*Golombek and Bridges*, 2000] for the observed dust particle size [*Tomasko et al.*, 1999; *Lemmon et al.*, 2004]. Deposition of 10^4 nm/yr would result in meters thick accumulations of dust within a comparatively short span of a million years. Because such accumulations are not observed at any of the landing sites, dust must be removed as rapidly as it is being deposited over relatively short timescales. This is particularly true at the Meridiani site, which has a very low albedo, indicating very little dust on the surface [*Golombek et al.*, 2005] even though the rover solar panels recorded these high deposition rates. Frequent dust devils observed at the Mars Pathfinder and Spirit landing sites as well as other dust cleaning events clearly play a role in the removal of dust from some surfaces. Analysis of dust devils observed by Spirit at Gusev crater showed they are easily capable of removing comparable amounts of dust from the surface with order 100 μm of dust removed during one dust devil season [*Greeley et al.*, 2006b].

[27] An environment in which liquid water is not stable is consistent with the very low erosion rates determined for the Late Hesperian and Amazonian and is also in accord with the lack of chemical weathering indicated by exposures of olivine basalt at Gusev [*McSween et al.*, 2004, 2006] and throughout equatorial Mars [*Hoefen et al.*, 2003; *Christensen et al.*, 2003]. Soils of Gusev and Meridiani [*Yen et al.*, 2005; *Christensen et al.*, 2004a, 2004b] as well as the atmospheric dust [*Goetz et al.*, 2005] are also basaltic and therefore have experienced limited aqueous alteration to form clays. These results do not necessarily contradict more recent wet conditions indicated by valley networks and gullies on Hesperian and Amazonian surfaces that may have been localized and over short periods [e.g., *Mangold et al.*, 2004; *Quantin et al.*, 2005; *Gulick and Baker*, 1990; *Malin and Edgett*, 2000b]. OMEGA results also show the atmospheric dust is not hydrated and thus has formed in the present dry environment [*Bibring et al.*, 2006]. Minor weathering rinds on basaltic rocks on the Gusev cratered plains are observed, as are concentrations of soluble elements and salts in near surface soils [*Yen et al.*, 2005; *Haskin et al.*, 2005], but both could have been accomplished via thin films of water under present climatic conditions [e.g., *Yen et al.*, 2005; *Hurowitz et al.*, 2006]. No evidence for liquid water interactions in exposed sulfate outcrop at Meridiani (e.g., leached surface salts) has been found [*Clark et al.*, 2005] and the observed pattern of crater gradation at Gusev and Meridiani shows no evidence for erosion by liquid water [*Grant et al.*, 2006a]. As a result, the dry and desiccating environment indicated by the very low erosion rates at both landing sites is supported by mineralogical and geochemical data throughout Mars that limits the role of liquid water since the Hesperian.

[28] By comparison, erosion rates estimated from changes in Noachian age crater distributions and morphologies on Mars (Table 1) are 3–5 orders of magnitude higher [*Craddock and Maxwell*, 1993; *Craddock et al.*, 1997; *Carr*, 1992; *Hynek and Phillips*, 2001; *Hartmann et al.*, 1999] than those derived from the landing sites and are comparable to slow denudation rates on the Earth (~5 B) that are dominated by liquid water [*Summerfield.*, 2005; *Saunders and Young*, 1983] (Figure 7). An estimate of the erosion rates applicable to Meridiani in the Late Noachian just prior to when the sulfates investigated by Opportunity were deposited is about 8 B, or 8,000 nm/yr from denudation in western Arabia Terra [*Hynek and Phillips*, 2001]. The Meridiani evaporites were deposited after this Late Noachian denudation event, and thus could represent the tail end of the wet climatic conditions in the latest Noachian or sporadically through the Hesperian on Mars [*Howard et al.*, 2005; *Irwin et al.*, 2005, and references therein].

[29] Erosion rates during the Noachian are ~5 orders of magnitude higher than those estimated for the Amazonian cratered plains of Gusev and are consistent with the wet and likely warm environment documented in Meridiani Planum during the Late Noachian. A wet environment in the Noachian is also indicated by the strong chemical and mineralogic evidence for aqueous processing of the older rocks of the Columbia Hills at Gusev crater [*Ming et al.*, 2006; *Morris et al.*, 2006; *Squyres et al.*, 2006]. The erosion rates from the Gusev cratered plains and Meridiani plains as well as those from Viking 1 and Pathfinder, limit this warmer and wetter period to before the Late Hesperian, around 3.5 Ga, and a dry and desiccating climate since. OMEGA results suggest that phyllosilicates formed in the presence of liquid water in the Noachian, sulfates formed in an acid aqueous environment in the Early Hesperian (~3.6 Ga), with a dry and desiccating environment since [*Bibring et al.*, 2006]. A wet Late Noachian period is also indicated by the age of valley network formation [*Baker et al.*, 1992; *Baker and Partridge*, 1986], layered sedimentary rocks, including the Meridiani sulfate evaporites [*Malin and Edgett*, 2000a; *Edgett*, 2005], as well as the timing of high erosion rates [*Grant and Schultz*, 1990, 1993; *Carr*, 1996; *Craddock et al.*, 1997; *Hynek and Phillips*, 2001] and may have been produced by outgassing associated with the formation of Tharsis [*Phillips et al.*, 2001].

7. Conclusions

[30] 1. An early warm and wet environment in the Late Noachian (>3.7 Ga) on Mars is indicated by Opportunity rover results on sulfate-rich "dirty" evaporites that were likely deposited in acid, saline interdune playas or sabkhas, roughly coeval with a wide variety of geomorphic indicators such as valley networks, degraded craters, highly eroded terrain, crater lakes and widespread layered sedimentary rocks.

[31] 2. Spirit's observations of the surficial geology of the Late Hesperian cratered volcanic plains at Gusev indicate that they were only modified by impact and lesser eolian activity. Localized eolian deflation of 5–27 cm of fines is indicated by two-toned rocks with a redder patination along their bases, ventifacts that originate from a common horizon above the surface, and perched and undercut rocks, and suggests eolian

redistribution of an equivalent amount of sediment to fill impact craters to form the ubiquitous hollows. This deflation yields the cumulative change of the surface since the plains were deposited in the Late Hesperian (~3.5 Ga) and yields an average erosion rate of ~0.03 nm/yr.

[32] 3. Slightly higher erosion rates (~1–10 nm/yr) are implied since the Hesperian at Meridiani Planum. Loss of Hesperian craters indicated by the sparsely cratered surface and Late Noachian age of the sulfates suggests 10–80 m of erosion. Modification and erosion of young, Late Amazonian craters by the saltating sand that progressively planes off ejecta blocks, back wastes and covers blocky rims with sand and granule ripples, and fills crater interiors with sand, indicates 1–10 m of erosion and redistribution of sand in the Late Amazonian (since ~0.4 Ga). Concentration of hematite concretions (''blueberries'') as a surface lag in the soils indicates 0.1–0.5 m of erosion. These higher erosion rates are consistent with eolian erosion of weak sulfates by saltating basaltic sand.

[33] 4. Long-term erosion rates of ~0.01–10 nm/yr since the Hesperian are consistent with erosion rates calculated in a similar manner for the Viking 1 and Mars Pathfinder landing sites and are 2–5 orders of magnitude lower than the slowest continental denudation rates on Earth. These erosion rates are so low that they preclude liquid water as an active erosional agent and argue for a dry and desiccating climate. Such a climate is also consistent with the lack of chemical weathering affecting olivine basalt; olivine basalt sand; basaltic, nonhydrated dust; the lack of salt leaching of exposed sulfates at Meridinai; and the lack of evidence for erosion by liquid water from the gradation of craters at both landing sites.

[34] 5. Erosion rates derived from previous studies of changes in Noachian age crater distributions and shapes and denudation of Terra Meridiani just before the sulfates were deposited are 2–5 orders of magnitude higher (10^3–10^4 nm/yr) than those from the Late Hesperian and Amazonian. These Noachian erosion rates are comparable to slow continental denudation rates on Earth that are dominated by liquid water. Erosion rates this high are consistent with a wet and warm environment in the Late Noachian and the deposition of sulfates at Meridiani Planum in salt water evaporitic playas or sabkhas.

[35] 6. Analyses of the geology and gradation histories of the landing sites and calculated erosion rates indicates the climatic change from wet and likely warm to dry and desiccating occurred sometime between the end of the Late Noachian and the beginning of the Late Hesperian or about 3.7–3.5 Ga.

[36] **Acknowledgments.** Research described in this paper was done by the MER project, Jet Propulsion Laboratory, California Institute of Technology, under a contract with NASA. This paper benefited from reviews by V. Baker and W. Goetz.

References

Arvidson, R., E. Guiness, and S. Lee (1979), Differential aeolian redistribution rates on Mars, *Nature*, *278*, 533–535.

Arvidson, R. E., et al. (2003), Mantled and exhumed terrains in Terra Meridiani, Mars, *J. Geophys. Res.*, *108*(E12), 8073, doi:10.1029/2002JE001982.

Arvidson, R. E., et al. (2004a), Localization and physical properties experiments conducted by Spirit at Gusev crater, *Science*, *305*, 821–824, doi:10.1126/science.1099922.

Arvidson, R. E., et al. (2004b), Localization and physical properties experiments conducted by Opportunity at Meridiani Planum, *Science*, *306*, 1730–1733, doi:10.1126/science.1104211.

Arvidson, R. E., et al. (2006a), Overview of the Spirit Mars Exploration Rover Mission to Gusev crater: Landing site to Backstay Rock in the Columbia Hills, *J. Geophys. Res.*, *111*, E02S01, doi:10.1029/2005JE002499.

Arvidson, R. E., et al. (2006b), Nature and origin of the hematite-bearing plains of Terra Meridiani based on analyses of orbital and Mars Exploration rover data sets, *J. Geophys. Res.*, *111*, E12S08, doi:10.1029/2006JE002728.

Baker, V. R., and J. B. Partridge (1986), Small Martian valleys: Pristine and degraded morphology, *J. Geophys. Res.*, *91*, 3561–3572.

Baker, V. R., M. H. Carr, V. C. Gulick, C. R. Williams, and M. S. Marley (1992), Channels and valley networks, in *Mars*, edited by H. H. Kieffer et al., pp. 493–522, Univ. of Ariz. Press, Tucson.

Bibring, J.-P., et al. (2006), Global mineralogical and aqueous Mars history derived from OMEGA/Mars Express data, *Science*, *312*, 400–404, doi:10.1126/science.1122659.

Bishop, P., and G. Goldrick (2000), Geomorphological evolution of the east Australia continental margin, in *Geomorphology and Global Tectonics*, edited by M. A. Summerfield, pp. 225–254, John Wiley, Hoboken, N. J.

Brown, R. W., K. Gallagher, A. J. W. Gleadow, and M. Summerfield (2000), Morphotectonic evolution of the South Atlantic margins of Africa and South America, in *Geomorphology and Global Tectonics*, edited by M. A. Summerfield, pp. 255–281, John Wiley, Hoboken, N. J.

Brown, R. W., M. A. Summerfield, and A. J. W. Gleadow (2002), Denudational history along a transect across the Drakensberg Escarpment of southern Africa derived from apatite fission track thermochronology, *J. Geophys. Res.*, *107*(B12), 2350, doi:10.1029/2001JB000745.

Cabrol, N. A., and E. A. Grin (1999), Distribution, classification and ages of Martian impact crater lakes, *Icarus*, *142*, 160–172.

Cabrol, N. A., E. A. Grin, R. Landheim, R. O. Kuzmin, and R. Greeley (1998a), Duration of the Ma'adim Vallis/Gusev crater hydrologic system, *Icarus*, *133*, 98–108.

Cabrol, N. A., E. A. Grin, and R. Landheim (1998b), Ma'adim Vallis evolution: Geometry and models of discharge rate, *Icarus*, *132*, 362–377.

Carr, M. H. (1992), Post-Noachian erosion rates: Implications for Mars climate change, *Lunar Planet. Sci.*, *XXIII*, 205–206.

Carr, M. H. (1996), *Water on Mars*, 229 pp., Oxford Univ. Press, New York.

Christensen, P. R., et al. (2003), Morphology and composition of the surface of Mars: Mars Odyssey THEMIS results, *Science*, *300*, 2056–2061, doi:10.1126/science.1080885.

Christensen, P. R., et al. (2004a), Mineralogy at Meridiani Planum from the Mini-TES experiment on the Opportunity rover, *Science*, *306*, 1733–1739.

Christensen, P. R., et al. (2004b), Initial results from the Miniature Thermal Emission Spectrometer experiment at the Spirit landing site at Gusev crater, *Science*, *305*, 837–842.

Clark, B. C., et al. (2005), Chemistry and mineralogy of outcrops at Meridiani Planum, *Earth Planet. Sci. Lett.*, *240*, 73–94, doi:10.1016/j.epsl.2005.09.040.

Craddock, R. A., and A. D. Howard (2002), The case for rainfall on a warm, wet early Mars, *J. Geophys. Res.*, *107*(E11), 5111, doi:10.1029/2001JE001505.

Craddock, R. A., and T. A. Maxwell (1993), Geomorphic evolution of the Martian highlands through ancient fluvial processes, *J. Geophys. Res.*, *98*, 3453–3468.

Craddock, R. A., T. A. Maxwell, and A. D. Howard (1997), Crater morphology and modification in the Sinus Sabaeus and Margaritifer Sinus regions of Mars, *J. Geophys. Res.*, *102*, 13,321–13,340.

Crumpler, L. S., et al. (2005), Mars Exploration Rover geologic traverse by the Spirit rover in the plains of Gusev crater, Mars, *Geology*, *33*(10), 809–812, doi:10.1130/G21673.1.

Edgett, K. S. (2005), The sedimentary rocks of Sinus Meridiani: Five key observations from data acquired by the Mars Global Surveyor and Mars Odyssey orbiters, *Mars*, *1*, 5–58, doi:10.1555/mars.2005.0002.

Fairbridge, R. W., and C. W. Finkl Jr. (1980), Cratonic erosional unconformities and peneplains, *J. Geol.*, *88*, 69–85.

Goetz, W., et al. (2005), Indication of drier periods on Mars from the chemistry and mineralogy of atmospheric dust, *Nature*, *436*, 62–65, doi:10.1038/nature03807.

Golombek, M. P., and N. T. Bridges (2000), Erosion rates on Mars and implications for climate change: Constraints from the Pathfinder landing site, *J. Geophys. Res.*, *105*, 1841–1853.

Golombek, M. P., et al. (2003), Selection of the Mars Exploration Rover landing sites, *J. Geophys. Res.*, *108*(E12), 8072, doi:10.1029/2003JE002074.

Golombek, M. P., et al. (2005), Assessment of Mars Exploration Rover landing site predictions, *Nature*, *436*, 44–48, doi:10.1038/nature03600.
Golombek, M. P., et al. (2006), Geology of the Gusev cratered plains from the Spirit rover transverse, *J. Geophys. Res.*, *111*, E02S07, doi:10.1029/2005JE002503.
Grant, J. A., and T. J. Parker (2002), Drainage evolution of the Margaritifer Sinus region, Mars, *J. Geophys. Res.*, *107*(E9), 5066, doi:10.1029/2001JE001678.
Grant, J. A., and P. H. Schultz (1990), Gradational epochs on Mars: Evidence from west-northwest of Isidis basin and Electris, *Icarus*, *84*, 166–195.
Grant, J. A., and P. H. Schultz (1993), Gradation of selected terrestrial and Martian impact craters, *J. Geophys. Res.*, *98*, 11,025–11,042.
Grant, J. A., et al. (2004), Surficial deposits at Gusev crater along Spirit rover traverses, *Science*, *305*, 807–810, doi:10.1126/science.1099849.
Grant, J. A., et al. (2006a), Crater gradation in Gusev crater and Meridiani Planum, Mars, *J. Geophys. Res.*, *111*, E02S08, doi:10.1029/2005JE002465.
Grant, J. A., S. A. Wilson, S. W. Ruff, M. P. Golombek, and D. L. Koestler (2006b), Distribution of rocks on the Gusev Plains and on Husband Hill, Mars, *Geophys. Res. Lett.*, *33*, L16202, doi:10.1029/2006GL026964.
Greeley, R., et al. (2004), Wind-related processes detected by the Spirit rover at Gusev crater, Mars, *Science*, *305*, 810–813, doi:10.1126/science.1100108.
Greeley, R., B. H. Foing, H. Y. McSween, G. Neukum, P. Pinet, M. van Kan, S. C. Werner, D. A. Williams, and T. E. Zegers (2005), Fluid lava flows in Gusev crater, Mars, *J. Geophys. Res.*, *110*, E05008, doi:10.1029/2005JE002401.
Greeley, R., et al. (2006a), Gusev crater: Wind-related features and processes observed by the Mars Exploration Rover Spirit, *J. Geophys. Res.*, *111*, E02S09, doi:10.1029/2005JE002491.
Greeley, R., et al. (2006b), Active dust devils in Gusev crater, Mars: Observations from the Mars Exploration Rover Spirit, *J. Geophys. Res.*, *111*, E12S09, doi:10.1029/2006JE002743.
Grotzinger, J. P., et al. (2005), Stratigraphy and sedimentology of a dry to wet eolian depositional system, Burns formation, Meridiani Planum, Mars, *Earth Planet. Sci. Lett.*, *240*, 11–72, doi:10.1016/j.epsl.2005.09.039.
Gulick, V. C., and V. R. Baker (1990), Origin and evolution of valleys on Martian volcanoes, *J. Geophys. Res.*, *95*, 14,325–14,344.
Haskin, L. A., et al. (2005), Water alteration of rocks and soils on Mars at the Spirit rover site in Gusev crater, *Nature*, *436*, 66–69, doi:10.1038/nature03640.
Hartmann, W. K., and G. Neukum (2001), Cratering chronology and evolution of Mars, *Space Sci. Rev.*, *96*, 165–194.
Hartmann, W. K., M. Malin, A. McEwen, M. Carr, L. Soderblom, P. Thomas, E. Danielson, P. James, and J. Veverka (1999), Evidence for recent volcanism on Mars from crater counts, *Nature*, *397*, 586–589.
Hoefen, T., R. N. Clark, J. L. Bandfield, M. D. Smith, J. C. Pearl, and P. R. Christensen (2003), Discovery of olivine in the Nili Fossae region of Mars, *Science*, *302*, 627–630.
Howard, A. D., J. M. Moore, and R. P. Irwin III (2005), An intense terminal epoch of widespread fluvial activity on early Mars: 1. Valley network incision and associated deposits, *J. Geophys. Res.*, *110*, E12S14, doi:10.1029/2005JE002459.
Hurowitz, J. A., S. M. McLennan, N. J. Tosca, R. E. Arvidson, J. R. Michalski, D. W. Ming, C. Schroder, and S. W. Squyres (2006), In situ and experimental evidence for acidic weathering of rocks and soils on Mars, *J. Geophys. Res.*, *111*, E02S19, doi:10.1029/2005JE002515.
Hynek, B. M. (2004), Implications for hydrologic processes on Mars from extensive bedrock outcrops throughout Terra Meridiani, *Nature*, *431*, 156–159.
Hynek, B. M., and R. J. Phillips (2001), Evidence for extensive denudation of the Martian highlands, *Geology*, *29*, 407–410.
Hynek, B. M., R. E. Arvidson, and R. J. Phillips (2002), Geologic setting and origin of Terra Meridiani hematite deposit on Mars, *J. Geophys. Res.*, *107*(E10), 5088, doi:10.1029/2002JE001891.
Irwin, R. P. I., T. A. Maxwell, A. D. Howard, R. A. Craddock, and D. W. Leverington (2002), A large paleolake basin at the head of Ma'adim Vallis, Mars, *Science*, *296*, 2209–2212.
Irwin, R. P., III, A. D. Howard, R. A. Craddock, and J. M. Moore (2005), An intense terminal epoch of widespread fluvial activity on early Mars: 2. Increased runoff and paleolake development, *J. Geophys. Res.*, *110*, E12S15, doi:10.1029/2005JE002460.
Judson, S., and D. F. Ritter (1964), Rates of regional denudation in the United States, *J. Geophys. Res.*, *69*, 3395–3401.
King, L. C. (1962), *The Morphology of the Earth*, Oliver and Boyd, White Plains, N. Y.
Kuzmin, R. O., R. Greeley, R. Landheim, N. A. Cabrol, and J. Farmer (2000), Geologic map of the MTM-15182 and MTM 15187 Quadrangles, Gusev crater-Ma'adim Valles region, Mars, *U. S. Geol. Surv. Misc. Invest. Map*, *I-2666*.
Landis, G. A., and P. P. Jenkins (2000), Measurement of the settling rate of atmospheric dust on Mars by the MAE instrument on Mars Pathfinder, *J. Geophys. Res.*, *105*, 1855–1857.
Lane, M. D., P. R. Christensen, and W. K. Hartmann (2003), Utilization of the THEMIS visible and infrared imaging data for crater population studies of the Meridiani Planum landing site, *Geophys. Res. Lett.*, *30*(14), 1770, doi:10.1029/2003GL017183.
Lemmon, M. T., et al. (2004), Atmospheric imaging results from the Mars Exploration Rovers: Spirit and Opportunity, *Science*, *306*, 1753–1756.
Malin, M. C., and K. S. Edgett (2000a), Sedimentary rocks of early Mars, *Science*, *290*, 1927–1937.
Malin, M. C., and K. S. Edgett (2000b), Evidence for recent groundwater seepage and surface runoff on Mars, *Science*, *288*, 2330–2335.
Malin, M. C., and K. S. Edgett (2003), Evidence for persistent flow and aqueous sedimentation on early Mars, *Science*, *302*, 1931–1934, doi:10.1126/science.1090544.
Mangold, N., C. Quantin, V. Ansan, C. Delacourt, and P. Allmand (2004), Evidence for precipitation on Mars from dendritic valleys in the Valles Marineris area, *Science*, *305*, 78–81.
Maxwell, T. A., and R. Irwin III (2004), The fate of channel deposits under shifting climate conditions on Earth and Mars, paper presented at Second Conference on Early Mars, Lunar and Planet. Inst., Jackson Hole, Wyo., 11–15 Oct.
McEwen, A. S., B. S. Preblich, E. P. Turtle, N. A. Artemieva, M. P. Golombek, M. Hurst, R. L. Kirk, D. M. Burr, and P. R. Christensen (2005), The rayed crater Zunil and interpretations of small impact craters on Mars, *Icarus*, *176*, 351–381.
McLennan, S. M., et al. (2005), Provenance and diagenesis of the evaporite-bearing Burns formation, Meridiani Planum, Mars, *Earth Planet. Sci. Lett.*, *240*, doi:10.1016/j.epsl.2005.09.041.
McSween, H. Y., et al. (2004), Basaltic rocks analyzed by the Spirit rover in Gusev crater, *Science*, *305*, 842–845.
McSween, H. Y., et al. (2006), Characterization and petrologic interpretation of olivine-rich basalts at Gusev crater, Mars, *J. Geophys. Res.*, *111*, E02S10, doi:10.1029/2005JE002477.
Ming, D. W., et al. (2006), Geochemical and mineralogical indicators for aqueous processes in the Columbia Hills of Gusev crater, Mars, *J. Geophys. Res.*, *111*, E02S12, doi:10.1029/2005JE002560.
Morris, R. V., et al. (2006), Mossbauer mineralogy of rock, soil, and dust at Gusev crater, Mars: Spirit's journey through weakly altered olivine basalt on the plains and pervasively altered basalt in the Columbia Hills, *J. Geophys. Res.*, *111*, E02S13, doi:10.1029/2005JE002584.
Phillips, R. J., et al. (2001), Ancient geodynamics and global-scale hydrology on Mars, *Science*, *291*, 2587–2591.
Pike, R. J. (1980), Control of crater morphology by gravity and target type: Mars, Earth, Moon, *Proc. Lunar Planet. Sci. Conf.*, *11th*, 2159–2189.
Quantin, C., P. Allemand, N. Mangold, G. Dromart, and C. Delacourt (2005), Fluvial and lacustrine activity on layered deposits in Melas Chasma, Valles Marineris, Mars, *J. Geophys. Res.*, *110*, E12S19, doi:10.1029/2005JE002440.
Ravine, M. A., and R. A. F. Grieve (1986), An analysis of morphologic variations in simple lunar craters, *Proc. Lunar Planet. Sci. Conf. 17th*, Part 1, *J. Geophys. Res.*, *91*, E75–E83.
Saunders, I., and A. Young (1983), Rates of surface processes on slopes, slope retreat and denudation, *Earth Surf. Processes Landforms*, *8*, 473–501.
Soderblom, L. A., et al. (2004), Soils of Eagle crater and Meridiani Planum at the Opportunity rover landing site, *Science*, *306*, 1723–1726, doi:10.1126/science.1105127.
Squyres, S. W., et al. (2004), In-situ evidence for an ancient aqueous environment on Mars, *Science*, *306*, 1709–1714.
Squyres, S. W., et al. (2006), Rocks of the Columbia Hills, *J. Geophys. Res.*, *111*, E02S11, doi:10.1029/2005JE002562.
Sullivan, R., et al. (2005), Aeolian processes at the Mars Exploration Rover Meridiani Planum landing site, *Nature*, *436*, 58–61, doi:10.1038/nature03641.
Summerfield, M. A. (2005), A tale of two scales, or the two geomorphologies, *Trans. Inst. Br. Geogr.*, *30*, 402–415.
Tanaka, K. L. (1986), The stratigraphy of Mars, *Proc. Lunar. Planet. Sci. Conf. 17th*, Part 1, *J. Geophys. Res.*, *91*, suppl., E139–E158.
Tanaka, K. L., J. A. Skinner Jr., T. M. Hare, T. Joyal, and A. Wenker (2003), Resurfacing history of the northern plains of Mars based on geologic mapping of Mars Global Surveyor data, *J. Geophys. Res.*, *108*(E4), 8043, doi:10.1029/2002JE001908.
Tanaka, K. L., J. A. Skinner Jr., and T. M. Hare (2005), Geologic map of the northern plains of Mars, *U.S. Geol. Surv. Sci. Invest. Map, SIM 2888*.
Tomasko, M. G., L. R. Doose, M. Lemmon, P. H. Smith, and E. Wegryn (1999), Properties of dust in the Martian atmosphere from the Imager for Mars Pathfinder, *J. Geophys. Res.*, *104*, 8987–9007.
Twidale, C. R. (1978), On the origin of Ayer's Rock, *Z. Geomorphol.*, *31*, 177–206.

Weitz, C. M., R. C. Anderson, J. F. Bell III, W. H. Farrand, K. E. Herkenhoff, J. R. Johnson, B. L. Jolliff, R. V. Morris, S. W. Squyres, and R. J. Sullivan (2006), Soil grain analyses at Meridiani Planum, Mars, *J. Geophys. Res.*, *111*, E12S04, doi:10.1029/2005JE002541.

Wood, C. A., and L. Andersson (1978), New morphometric data for fresh lunar craters, *Proc. Lunar Planet. Sci. Conf.*, *9th*, 3669–3689.

Yen, A. S., et al. (2005), An integrated view of the chemistry and mineralogy of Martian soils, *Nature*, *436*, 49–54, doi:10.1038/nature03637.

Young, R. W. (1983), The tempo of geomorphological change, *J. Geol.*, *91*, 221–230.

R. E. Arvidson, Department of Earth and Planetary Sciences, Washington University, Campus Box 1169, One Brookings Drive, St. Louis, MO 63130, USA.

J. F. Bell III, S. W. Squyres, and R. Sullivan, Department of Astronomy, Cornell University, Ithaca, NY 14853, USA.

P. R. Christensen and R. Greeley, Department of Geological Sciences, Arizona State University, Tempe, AZ 85287, USA.

L. S. Crumpler, New Mexico Museum of Natural History and Science, 1801 Mountain Road NW, Albuquerque, NM 87104, USA.

M. P. Golombek, Jet Propulsion Laboratory, California Institute of Technology, Pasadena, CA 91109, USA. (mgolombek@jpl.nasa.gov)

J. A. Grant, Center for Earth and Planetary Studies, National Air and Space Museum, Smithsonian Institution, 6th and Independence SW, Washington, DC 20560, USA.

L. A. Soderblom, U. S. Geological Survey, 2255 North Gemini Drive, Flagstaff, AZ 86001, USA.

C. M. Weitz, Planetary Science Institute, 1700 East Fort Lowell, Suite 106, Tucson, AZ 85719, USA.